

Marginal conditions of thermoacoustic Taconis oscillations revisited

Dai Shimizu (1) and Nobumasa Sugimoto (2)

(1) Creative Design Studio on Technology, Graduate School of Engineering, University of Osaka, Suita, Osaka 565-0871, Japan

(2) Department of Mechanical Science, Graduate School of Engineering Science, University of Osaka, Toyonaka, Osaka 560-8531, Japan

PACS: 43.35.Ud, 47.35.Rs, 47.15.Cb

ABSTRACT

This paper revisits derivation of marginal conditions for the onset of thermoacoustic Taconis oscillations in a helium-filled, quarter-wavelength tube. For step temperature distributions, the linear stability analysis is made by Rott (1969, 1973) and the marginal conditions derived are experimentally checked by Yazaki, Tominaga, and Narahara (1980). Although the boundary-layer theory was then regarded as being incapable of deriving the conditions, it has recently been revealed that the theory is valid in any situation for a short-time behavior after a disturbance is given. Therefore it is expected to be applicable for derivation of the marginal conditions. Using this theory, marginal conditions for *smooth* temperature distribution are sought and they are checked against the results by Rott.

INTRODUCTION

The Taconis oscillations are known as a prototype of thermoacoustic oscillations resulting from instability of gas in contact with a wall subjected to temperature gradient. They occur in a helium-filled, quarter-wavelength tube with its open end cooled down to the cryogenic temperature and closed end kept at room temperature. Given a geometry of the tube and a temperature distribution along it, marginal conditions of instability are specified for the temperature ratio at the closed end to that of the open one against the tube radius relative to the thickness of diffusion layer.

The marginal conditions are derived by Rott (1969); Rott (1973) for step temperature distribution. Later the curves are checked experimentally by Yazaki, Tominaga, and Narahara (1980) and good agreements are observed. In developing the theory, Rott regarded the boundary-layer theory, first-order theory in thickness of the layer, as being incapable of deriving the conditions. But it has recently been shown that it is applicable to simulation of the Taconis oscillations (Sugimoto and Shimizu 2008). Extending the theory to a weakly nonlinear case, in fact, they have succeeded in simulating initial instability of a disturbance and ensuing emergence of self-excited oscillations, and in unveiling the mechanisms of them (Shimizu and Sugimoto 2009; Shimizu and Sugimoto 2010).

But there has been left a problem to confirm whether or not the marginal curves are available by the boundary-layer theory. Thus the purpose of this paper is to obtain marginal conditions by using the boundary-layer theory and to check them with the theoretical results by Rott. To this end, the linearized equations have only to be solved. But since the numerical code to solve the nonlinear equations is now available, initial-value problems to them are solved.

FUNDAMENTAL EQUATIONS

Frequency equation by Rott

First of all, Rott's theory is reproduced briefly. All basic equations are linearized by assuming that a tube radius is narrow

enough in comparison with a tube length and a typical axial length involved in the temperature gradient. This approximation has a great merit, which allows us to regard the pressure as being uniform over a cross-section of the tube. But it is obvious that this assumption breaks down near the step.

For a harmonic disturbance having an angular frequency ω , the following equation for the complex amplitude P of an excess pressure is derived by using the assumption that the pressure is uniform over a cross-section of the tube:

$$[1 + (\gamma - 1)f^*]P + \frac{d}{dx} \left[\frac{a^2}{\omega^2} (1 - f) \frac{dP}{dx} \right] - \frac{a^2}{\omega^2} \frac{f^* - f}{1 - \text{Pr}} \frac{1}{T} \frac{dT}{dx} \frac{dP}{dx} = 0, \quad (1)$$

with

$$f(\eta) = \frac{2J_1(i\eta)}{i\eta J_0(i\eta)}, \quad f^* = f(\eta\sqrt{\text{Pr}}), \quad \eta = R \left(\frac{i\omega}{\nu} \right)^{1/2}, \quad (2)$$

where x , t and T denote, respectively, the axial coordinate along the tube, the time and the wall temperature; J_0 and J_1 denote, respectively, Bessel functions of the zeroth and first order; γ , Pr and R denote, respectively, ratio of specific heats, Prandtl number and a tube radius; a and ν denote, respectively, a local adiabatic sound speed and a kinematic viscosity. Temperature dependence of the shear viscosity is taken into account in the form of a power law of the temperature T as T^β , β being a constant 0.647.

For the step distribution, $T^{-1}dT/dx$ diverges locally. Rott managed to remove this singularity by transforming Eq. (1) into two equivalent equations so that the third term may disappear. Then the problem is reduced to the determination of matching conditions between two solutions in cold and hot parts. Then the frequency equation is given as follows:

$$G_c \frac{\cot(\lambda_c h_c)}{\xi \lambda_c h_c} = G_h \frac{\tan(\lambda_h h_h)}{\lambda_h h_h}, \quad (3)$$

with

$$G = [1 + (\gamma - 1)f^*] \exp \left\{ - \int \frac{f^* - f}{(1 - \text{Pr})(1 - f)} \theta dx \right\}, \quad (4)$$

and

$$\lambda_c = \frac{\omega l}{a_c}, \lambda_h = \frac{\omega(L-l)}{a_h}, \xi = \frac{L-l}{l}, h = \left(\frac{1 + (\gamma - 1)f^*}{1 - f} \right)^{1/2}, \quad (5)$$

where the subscript c and h denote, respectively, values in the cold and hot parts; L and l denote, respectively, a tube length and a distance from the open end ($x = 0$) to the step. The marginal conditions are obtained as shown in Fig. 3 and Fig. 4 in Rott (1973) by expansions of Eq. (3) up to the order of ε^2 where $\varepsilon = 2/\eta$.

Formulation of the boundary-layer theory

The boundary-layer theory developed by Sugimoto and Shimizu (2008) is briefly outlined. It is based on the assumption that thermoviscous diffusion layer is confined to a narrow region on the tube wall. Dividing a field in the tube into a boundary-layer and an acoustic main-flow region outside of it, the boundary layer is assumed to be described by the linear and first-order theory in its thickness. Fluid-dynamical equations are averaged over the cross-section of the tube, from which one-dimensional equations over the main-flow region are derived by using the boundary-layer solutions.

The system of equations thus obtained is given as follows:

$$\frac{1}{\gamma(p_0 + p')} \left(\frac{\partial p'}{\partial t} + u' \frac{\partial p'}{\partial x} \right) + \frac{\partial u'}{\partial x} = \frac{2}{R} v_b, \quad (6)$$

$$\frac{\partial u'}{\partial t} + u' \frac{\partial u'}{\partial x} = - \frac{1}{\rho_e + \rho'} \left(\frac{\partial p'}{\partial x} - F \right), \quad (7)$$

$$\frac{\partial S'}{\partial t} + u' \left(\frac{dS_e}{dx} + \frac{\partial S'}{\partial x} \right) = 0, \quad (8)$$

$$\frac{\rho'}{\rho_e} = \left(\frac{p_0 + p'}{p_0} \right)^{1/\gamma} \exp \left(- \frac{S'}{c_p} \right) - 1, \quad (9)$$

where p' , u' , ρ' and S' denote, respectively, disturbance in the pressure, axial velocity, density and entropy from the respective equilibrium values given by p_0 , 0, $\rho_e(x)$ and $S_e(x)$, the subscript e implying the equilibrium.

Here v_b on the right-hand side of Eq. (6) represents the velocity at the edge of the boundary layer directed normal to the tube wall and into the main-flow region, which is given by

$$v_b = \sqrt{v_e} \left(- \frac{C}{\rho_e a_e^2} \frac{\partial^{\frac{1}{2}} p'}{\partial t^{\frac{1}{2}}} + \frac{C_T}{T_e} \frac{dT_e}{dx} \frac{\partial^{-\frac{1}{2}} u'}{\partial t^{-\frac{1}{2}}} \right), \quad (10)$$

with the definitions of the plus and minus half-order derivatives (Gel'fand and Shilov 1964):

$$\frac{\partial^{\pm \frac{1}{2}} p'}{\partial t^{\pm \frac{1}{2}}} = \frac{1}{\sqrt{\pi}} \int_{-\infty}^t \frac{1}{\sqrt{t-\tau}} \frac{\partial^{\frac{1}{2} \pm \frac{1}{2}} p'(x, \tau)}{\partial \tau^{\frac{1}{2} \pm \frac{1}{2}}} d\tau, \quad (11)$$

the sign \pm vertically ordered, where $C = 1 + (\gamma - 1)/\sqrt{\text{Pr}}$ and $C_T = (1 + \beta)/2 + 1/(\sqrt{\text{Pr}} + \text{Pr})$ (Sugimoto 2010), a_e being an adiabatic sound speed. Here the power-law for the viscosity is also assumed, though it has been neglected in the previous papers for simplicity. On the right-hand side of Eq. (7), $F(x, t)$ denotes an impulsive force per unit volume to cope with an initial condition. It decreases rapidly as the time elapses.

Effects of the boundary layer appear through the memory integrals expressed in terms of both half-order derivatives. For a

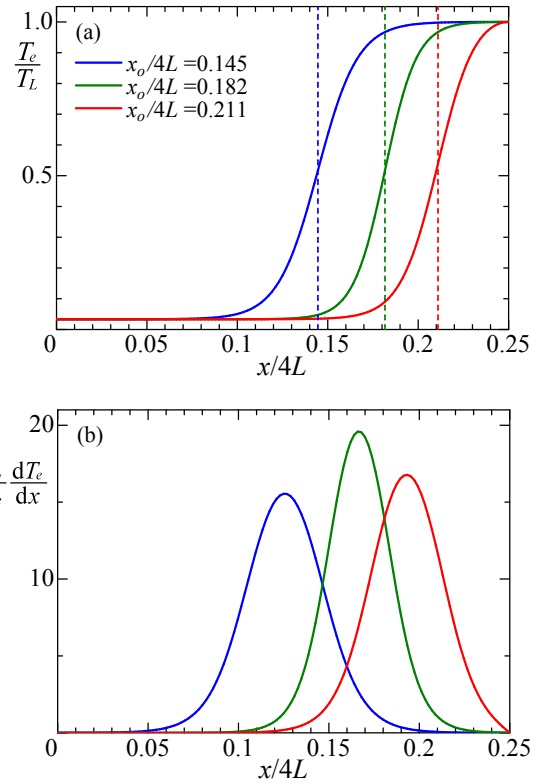


Figure 1: Axial distributions of temperature $T_e(x)$ relative to T_L at $x = L$ and gradient of the logarithmic temperature $T_e^{-1} dT_e/dx$ for $x_o/4L(= 0.211, 0.182$ and $0.145)$ and for the tube lengths $L = 1, 1.26$ and 1.07 m, respectively, where the temperature ratio is fixed at $n = 30$. The broken lines in (a) indicate the axial positions of the maximum gradient of T_e at $x = x_o$, which are different from the ones for the maximum of $T_e^{-1} dT_e/dx$ in (b).

smooth temperature distribution increasing monotonically toward the closed end, the one-dimensional equations (6)-(11) are solved numerically by imposing initial and boundary conditions as follows:

$$p' = 0 \text{ and } u' = \varepsilon a_L \cos \left(\frac{\pi x}{2L} \right), \quad (12)$$

at $t = 0+$ in the interval $0 < x < L$, with $p' = u' = 0$ for $t < 0$ where ε measures an acoustic Mach number referenced to the sound speed a_L at the closed end, and

$$p' = 0 \text{ at } x = 0, \quad (13)$$

$$u' = (C - 1) \frac{\sqrt{v_e}}{\rho_e a_e^2} \frac{\partial^{\frac{1}{2}} p'}{\partial t^{\frac{1}{2}}} \text{ at } x = L, \quad (14)$$

for $t > 0$, where radiation from the open end is neglected so that required is the excess pressure to vanish at the open end, while the boundary layer at the closed end is taken into account for the axial velocity.

NUMERICAL SIMULATIONS

Smooth step temperature distributions

Marginal conditions are derived by the analysis of linear stability assuming infinitesimally small disturbance, which is supposed to be imposed as $t \rightarrow -\infty$. In numerical simulations by solving the nonlinear equations (6)-(9), however, a disturbance of *finite* magnitude, no matter how small it may be, must be imposed at a *finite* time. In this sense, strictly speaking, conditions obtained theoretically are not equivalent to those numerically. But taking a very small disturbance, i.e. the value of ε , this difference is expected to be diminished.

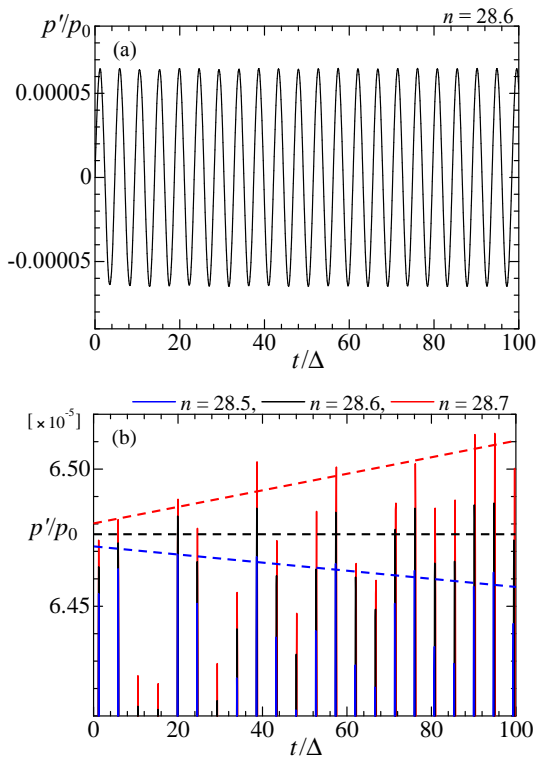


Figure 2: Temporal variations of the excess pressure p' relative to p_0 at the closed end for $\xi = 1.0$ with $R = 10$ mm, where (a) shows the marginal case for $n = 28.6$ and (b) shows the cases for $n = 28.5$, $n = 28.6$ and $n = 28.7$ with trend lines shown in broken lines for the maxima in each cycle of oscillations.

Because a step temperature distribution is not realistic, a smooth temperature distribution is assumed for T_e , which is taken to be the combination of hyperbolic functions as:

$$\frac{T_e(x)}{T_L} = \frac{G(x) - G(0)}{1 - G(0)} + \frac{1}{n} \left[\frac{1 - G(x)}{1 - G(0)} \right], \quad (15)$$

with

$$G(x) = \frac{D(x) + D(2L - x) - 1}{2D(L) - 1}, \quad (16)$$

and

$$D(x) = \frac{1}{2} \tanh[\alpha(x - x_o)] - \frac{1}{2} \tanh[\alpha(x + x_o)] + 1, \quad (17)$$

where $G(L) = 1$ and $n (\geq 1)$ denotes the ratio of the temperature at the closed end to the one at the open end, α and x_o ($0 < x_o < L$) being positive constants.

The marginal conditions for the step are specified in terms of a position of the step through a parameter ξ ($= (L - l)/L$), where l denotes a distance of the step from the open end. For the smooth temperature distribution, however, this is not defined. For comparison, two choices are conceivable for l . One is to take a position for dT_e/dx to take a maximum, i.e. $x = x_o$, whereas the other to take a position for the gradient of the logarithmic temperature $T_e^{-1}dT_e/dx$ ($= d \log T_e/dx$) to take a maximum, as suggested by the form of v_b . As the limit to the step is taken, both maxima tend to coincide with each other.

In Fig. 1 (a) and (b), axial distributions of the temperature T_e and the gradient of the logarithmic temperature $T_e^{-1}dT_e/dx$ are shown for three values of x_o ($= 0.211, 0.182$ and 0.145) and for the tube lengths $L = 1, 1.26$ and 1.07 m, respectively, where the temperature ratio is fixed at $n = 30$. The tube lengths are taken

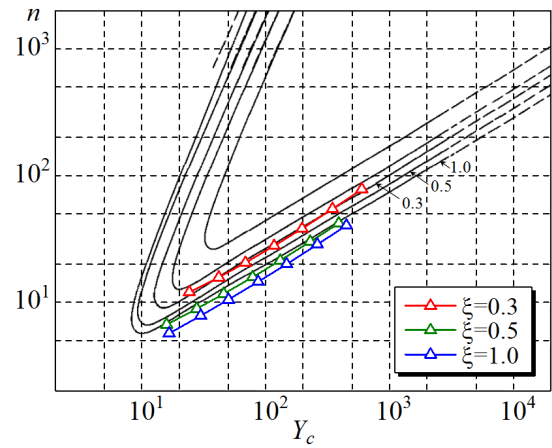


Figure 3: Marginal temperature ratio n versus $Y_c = R(\omega/v_c)^{1/2}$ for $\xi = 0.3, 0.5$ and 1.0 and for seven tubes of radius $R = 14, 10, 7, 5, 3.5, 2.5$ and 1.7 mm. The black solid and black broken lines are the marginal curves shown in Fig. 3 of Rott (1973).

to be the same as used by Yazaki, Tominaga, and Narahara (1980). As a result of trials of numerical calculations, it has been found that l is taken to be the distance to the position for the maximum of $T_e^{-1}dT_e/dx$ rather than x_o in view of better agreements with the marginal conditions for the step. By this choice, the values of x_o above are determined for ξ so as to take the value 0.3, 0.5 and 1.0, respectively.

Results and discussions

Numerical calculations are carried out by solving Eqs. (6)-(9) for $\xi = 0.3, 0.5$ and 1.0 , and for seven tubes of radius $R = 14, 10, 7, 5, 3.5, 2.5$ and 1.7 mm. The acoustic Mach number is chosen to be 10^{-5} so that the linear oscillations may be assumed. To seek a marginal temperature ratio, a maximum of p' in each cycle of oscillations is checked over ten to thirty periods from the initial state. In Fig. 2 (a), temporal variations of the excess pressure p' relative to p_0 at the closed end are shown for $n = 28.6$ and $\xi = 1.0$ with $R = 10$ mm, where $\Delta = 4L/a_L$. This case appears to be marginal but the amplitude fluctuates about the mean value slightly. As a criterion to identify the marginal temperature ratio, no change in the mean value is required. In the present calculations, this ratio is determined by sight up to the first three digits as shown in Figure 2 (b).

Figure 3 shows the marginal conditions obtained numerically are plotted on the marginal curves obtained by Rott for three values of ξ , where the black solid and broken lines are copied from the marginal curves shown in Fig. 3 in Rott (1973). It is seen that the marginal conditions sought numerically are close to the curves by Rott, especially when $\xi = 0.3$.

Thus the right branches of the marginal curves for the step are confirmed by the boundary-layer theory but no left branches have been available. The marginal conditions obtained for $\xi = 0.3$ lie just on the curve but those for $\xi = 0.5$ and $\xi = 1$ lie below the curves. As ξ decreases, i.e. the cold part increases relatively in the tube, the marginal conditions obtained show good agreements with the results of Rott. A reason of this is explained as follows.

Figure 4 (a) shows spatial profiles of the velocity at the edge of the boundary layer v_b relative to a_L in the case with $\xi = 1$ and $n = 28.6$ for the tube $R = 10$ mm, i.e. for the same conditions of Fig. 2 (a). Here the profiles are taken at every 1/16th period of the oscillations from $t/\Delta = 51.52$ to 56.20 . For a reference, the excess pressure p' relative to p_0 for the same period of the

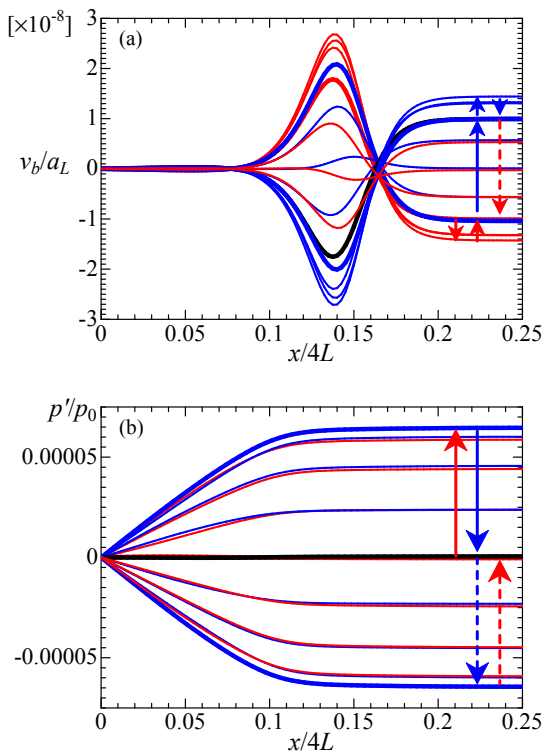


Figure 4: Spatial profiles of the velocity at the edge of the boundary layer v_b relative to a_L and the excess pressure p' relative to p_0 at every 1/16th period of the oscillations from $t/\Delta = 51.52$ to 56.20 for $n = 28.6$ and $\xi = 1.0$ with $R = 10$ mm

oscillations are also shown in (b). It is found from Fig. 4 (a) that the variation of v_b in the cold part is very small in comparison with that in the hot part. It varies significantly near the center of the tube where the gradient of the logarithmic temperature takes maximum. Thus as the cold part becomes wider, there will increase a region for the boundary-layer approximation to be valid. This may be the reason of the good agreement in the case of the small value of ξ .

As ξ increases to approach unity, the marginal temperature numerically obtained lie below the marginal curves by Rott.

Since the curves for the step are expected to be lower than the ones for the smooth distribution, this discrepancy will be attributed to use of the first-order theory in the boundary-layer thickness.

CONCLUSIONS

The marginal conditions for the onset of the Taconis oscillations obtained analytically by Rott have been examined by a new approach based on the boundary-layer theory. It has been revealed that the right branch of the marginal curves is available for plausible values of the temperature ratio but no left branches are available yet. In particular, good agreements are observed quantitatively when a position of the step is chosen, for the smooth distribution, to be the one for the gradient of the logarithmic temperature to take a maximum. As far as the right branch of the marginal curves is concerned, the validity of the assumption of the step is endorsed by the present results for the smooth temperature distribution, while usefulness of the boundary-layer theory is also confirmed.

REFERENCES

- Gel'fand, I. M. and G. E. Shilov (1964). *Generalized functions Vol. 1*. New York: Academic Press, p. 117.
- Rott, N. (1969). "Damped and thermally driven acoustic oscillations in wide and narrow tubes". *Z. Angew. Math. Phys.* 20, pp. 230–243.
- (1973). "Thermally driven acoustic oscillations, Part II: stability limit for helium". *Z. Angew. Math. Phys.* 24, pp. 54–72.
- Shimizu, D. and N. Sugimoto (2009). "Physical Mechanisms of Thermoacoustic Taconis Oscillations". *J. Phys. Soc. Jpn.* 78, pp. 094401 1–6.
- (2010). "Numerical study of thermoacoustic Taconis oscillations". *J. Appl. Phys.* 107, pp. 034910 1–11.
- Sugimoto, N. (2010). "Thermoacoustic wave propagation in a narrow channel subject to temperature gradient". *ICA2010*.
- Sugimoto, N. and D. Shimizu (2008). "Boundary-layer theory for Taconis oscillations in a helium-filled tube". *Phys. Fluids* 20, pp. 104102 1–11.
- Yazaki, T., A. Tominaga, and Y. Narahara (1980). "Experiments on Thermally Driven Acoustic Oscillations of Gaseous Helium". *J. Low Temp. Phys.* 41, pp. 45–60.